Conference materials
UDC 538.9
DOI: https://doi.org/10.18721/JPM.161.102

TEM study of the defect structure of α-Ga_2O_3 layers grown by HVPE

A.V. Myasoedov [1]✉, I.S. Pavlov [2], A.I. Pechnikov [1,3],
S.I. Stepanov [1,3], V.I. Nikolaev [1,3]

[1] Ioffe Institute, Saint Petersburg, Russia;

[2] National Research Centre "Kurchatov Institute", Shubnikov Institute of Crystallography of Federal Scientific Research Centre "Crystallography and Photonics" of RAS, Moscow, Russia;

[3] Perfect Crystals LLC, Saint Petersburg, Russia

✉ amyasoedov88@gmail.com

Abstract. Prismatic stacking faults in α-Ga_2O_3 films on (0001) Al_2O_3 substrates are investigated using transmission electron microscopy (TEM). The studied films are grown by halide vapor phase epitaxy (HVPE) up to 1.3 μm in thickness. The initial growth stage results in threading dislocations (TDs) of an average density of 10^{10} cm^{-2}. The majority of the TDs are identified as 1/3 < $1\bar{1}00$ > partial edge and 1/3 < $1\bar{1}01$ > perfect mixed types using $\boldsymbol{g}\cdot\boldsymbol{b} = 0$ invisibility criterion under two-beam diffraction conditions. The edge component of Burgers vector is determined by the Burgers circuit procedure using high-resolution TEM images of dislocation cores. It is suggested that 1/3 < $1\bar{1}01$ > partial dislocations may arise as a result of dissociation of 1/3 < $2\bar{1}\bar{1}0$ > erfect dislocations which leads to the emergence of prismatic stacking faults in the films.

Keywords: gallium oxide, TEM, dislocations

Funding: This research was supported by the Russian Foundation for Basic Research (RFBR), grant No. 19-29-12041mk.

Citation: Myasoedov A.V., Pavlov I.S., Pechnikov A.I., Stepanov S.I., Nikolaev V.I. TEM study of the defect structure of α-Ga_2O_3 layers grown by HVPE, St. Petersburg State Polytechnical University Journal. Physics and Mathematics. 16 (1.1) (2023) 16–21. DOI: https://doi.org/10.18721/JPM.161.102

Материалы конференции
УДК 538.9
DOI: https://doi.org/10.18721/JPM.161.102

ПЭМ-исследование дефектной структуры пленок α-Ga_2O_3, выращенных методом хлоридной эпитаксии

А.В. Мясоедов [1]✉, И.С. Павлов [2], А.И. Печников [1,3],
С.И. Степанов [1,3], В.И. Николаев [1,3]

[1] Физико-технический институт им. А.Ф. Иоффе РАН, Санкт-Петербург, Россия;

[2] Национальный исследовательский центр «Курчатовский институт», Институт кристаллографии им. А.В. Шубникова ФНИЦ «Кристаллография и фотоника» РАН, Москва, Россия;

[3] ООО «Совершенные кристаллы», Санкт-Петербург, Россия

✉ amyasoedov88@gmail.com

Аннотация. Методом просвечивающей электронной микроскопии (ПЭМ) исследованы призматические дефекты упаковки в пленках α-Ga_2O_3 на (0001) Al_2O_3. Исследуемые пленки толщиной до 1,3 мкм были выращены методом хлоридной эпитаксии (ХЭ). Начальный этап эпитаксии сопровождается образованием высокой плотности проникающих дислокаций (ПД) на уровне 10^{10} см$^{-2}$. С помощью применения критерия невидимости $\boldsymbol{g} \cdot \boldsymbol{b} = 0$ при двухлучевых дифракционных условиях большинство ПД были определены как частичные $1/3 < 1\bar{1}00 >$ краевые и $1/3 < 1\bar{1}01 >$ дислокации смешанного типа. Краевая компонента была определена с помощью построения контура Бюргерса на изображениях высокого разрешения ядер дислокаций. Предполагается, что $1/3 < 1\bar{1}00 >$ частичные дислокации могут возникать в результате диссоциации $1/3 < 2\bar{1}\bar{1}0 >$ полных дислокаций, которая приводит к появлению призматических дефектов упаковки в пленке.

Ключевые слова: оксид галлия, ПЭМ, дислокации

Финансирование: Работа выполнена при поддержке РФФИ. Грант № 19 29 12041мк.

Ссылка при цитировании: Мясоедов А.В., Павлов И.С., Печников А.И., Степанов С.И., Николаев В.И. ПЭМ-исследование дефектной структуры пленок α-Ga_2O_3, выращенных методом хлоридной эпитаксии // Научно-технические ведомости СПбГПУ. Физико-математические науки. 2023. Т. 16. № 1.1. С. 16–21. DOI: https://doi.org/10.18721/JPM.161.102

Introduction

Gallium oxide (Ga_2O_3), a wide bandgap semiconductor, is an attractive material for applications in power and optoelectronic devices [1]. In recent years, much attention has been given to various polymorphs of Ga_2O_3. Among all polymorphic forms, α-Ga_2O_3 has the widest direct bandgap of 5–5.3 eV at room temperature. α-Ga_2O_3 devices have the potential to outperform current GaN devices [2]. This polymorph has the corundum crystal structure which allows to grow α-Ga_2O_3 on (0001) Al_2O_3 substrates by various techniques such as halide vapor phase epitaxy (HVPE) [3, 4]. However, the large lattice mismatch (~ 4.7%) between the epilayer and the substrate results in a high density of threading dislocations (TDs) in the order of 10^{10}–10^{11} cm^{-2} [5]. TDs propagate along the film growth direction <0001>. Numerous reports provided evidence that edge-type dislocations comprise the great majority of TDs in thin films of about 2 μm thickness [3, 5, 6]. TDs act as non-radiative and charged scattering centers, and negatively affect recombination efficiency and carrier mobility [7].

Revealing dislocations of different types is important for the optimization of the growth process and device design. In previous studies of monoclinic β-Ga_2O_3 single crystals, several possible slip systems, and more than 10 possible Burgers vectors of dislocations were characterized [8, 9]. It was determined by TEM analysis that, in addition to perfect dislocations, partial dislocations exist in β-Ga_2O_3 [9]. However, the character of dislocations in trigonal α-Ga_2O_3 is poorly described in the literature.

In this work, we investigate the dislocation structure in up to 1.3 μm thick α-Ga_2O_3 films grown by HVPE on (0001) sapphire substrates.

Materials and Methods

Single crystalline α-Ga_2O_3 films were grown on c-plane sapphire substrates by HVPE in an atmospheric pressure horizontal quartz reactor developed by Perfect Crystals LLC [10]. Gallium chloride (GaCl) and high-purity grade oxygen (O_2) were used as precursors. GaCl was synthesized in situ by passing gaseous hydrogen chloride (HCl) over metallic gallium (Ga) at 600 °C. The purity of HCl and Ga precursors was greater than 99.999%. The GaCl vapor was then mixed with O_2 in the deposition zone of the reactor to produce α-Ga_2O_3. The rate of deposition on a (0001) sapphire substrate varied from 8 to 12 μm·h^{-1}. The deposition duration was chosen to produce a layer with the desired thickness. The films were transparent, mirror like, and crack-free. Samples with a thickness of 0.8–1.3 μm were selected for the TEM study. According to our results, samples with different thicknesses showed similar results.

The TEM studies were carried out using an FEI Tecnai Osiris transmission electron microscope operated at 200 kV. Cross-sectional and plan-view lamellas were prepared using a conventional (lift-out) focused ion beam technique.

Results and Discussion

Typically, α-Ga_2O_3 films on Al_2O_3 substrates exhibit a high density of TDs. Fig. 1 shows dark-field (DF) cross-sectional TEM images, taken at different diffraction conditions. TDs are visible as line-shaped features that produce a diffraction contrast. According to earlier studies [5, 6], the great majority of TDs consist of edge-type dislocations. Moreover, edge dislocations are represented by two types, appearing in a ratio of 95 to 3.5%, has been recently described [11].

Our analysis of the dislocation structure in α-Ga_2O_3 films is mostly based on the geometry of slip systems determined for sapphire single crystals [12]. Table 1 summarizes the shortest Burgers vectors ***b*** and slip planes, available in sapphire crystals. The extension of this analysis to α-Ga_2O_3 is valid, because ***b*** values are similar to those of the established Burgers vectors of dislocations in α-Ga_2O_3 crystals. For the sake of convenience, we consider the Burgers vector to consist of two components lying perpendicular (*c*) and parallel (*a*) to the basal plane of the hexagonal lattice. It allows identifying dislocations using geometrically simply interpretable images.

Table 1

Shortest Burgers vectors and dislocation slip systems in Al_2O_3 and α-Ga_2O_3

Burgers vector	α-Ga_2O_3, Å	Al_2O_3, Å	Slip planes [12]
$1/3<11\bar{2}0>$	4.98	4.75	$(0001),(1\bar{1}00),(1\bar{1}01),(1\bar{1}02)$
$1/3<1\bar{1}01>$	5.32	5.12	$\{11\bar{2}0\},\{\bar{1}101\},\{\bar{1}102\},\{\bar{2}113\}$
$<1\bar{1}00>$	8.63	8.22	$\{0001\},\{11\bar{2}0\},\{11\bar{2}2\},\{11\bar{2}3\}$
$1/3<1\bar{1}00>$*	2.88	2.74	* Partial dislocation

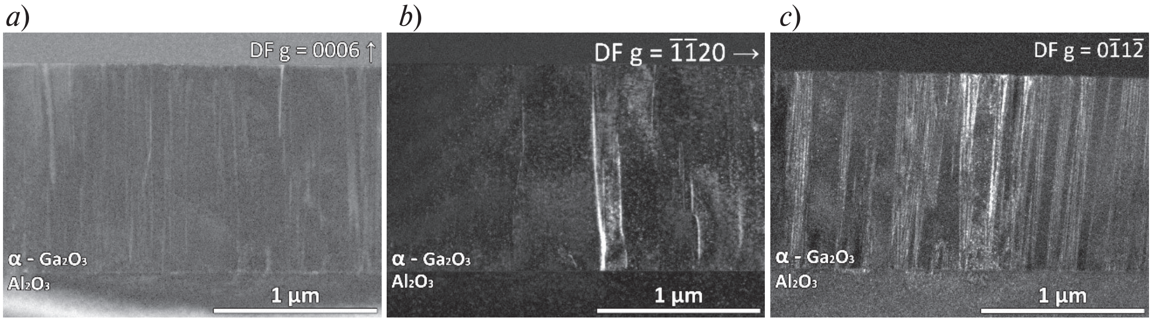

Fig. 1. Dark field TEM images of the cross-sectional area of α-Ga_2O_3 film with a thickness of 1.3 μm, acquired in two-beam diffraction conditions. The diffraction vector equals: ***g*** = 0006 (*a*); ***g*** = $\bar{1}\bar{1}20$ (*b*); ***g*** = $0\bar{1}12$ (*c*)

An edge-type TD has a non-zero ***a***-component and zero ***c***-component. In crystals with the corundum structure, there are two possible Burgers vectors that satisfy these conditions for perfect dislocations. They are indicated as $\boldsymbol{b}_1 = <11\bar{2}0>$ and $\boldsymbol{b}_2 = <1\bar{1}00>$ in Table 1. We note that the latter vector $\boldsymbol{b}_2$ is about twice the magnitude of the former. Therefore, the vector $\boldsymbol{b}_2$ can be disregarded from further consideration because it is unlikely to occur in α-Ga_2O_3. In addition, dislocations with the Burgers vector ***b*** = $<0001>$ have not been reported for sapphire crystals. Similarly, one could hardly expect to find a perfect screw TD in α-Ga_2O_3. At the same time, perfect mixed TDs that have non-zero ***a***- and ***c***-components are likely to be found in α-Ga_2O_3. The lowest magnitude of the Burgers vector, which satisfies this condition is ***b*** = $1/3<1\bar{1}00>$ (Table 1). It is consistent with experimental observations made for GaN. Perfect screw TDs with ***b*** = $<0001>$ are rare in GaN thin films, while mixed ones with ***b*** = $1/3<11\bar{2}3>$ are more common.

Lattice defects can be identified using the diffraction contrast. Variations in the dislocation visibility can be interpreted using the well-known invisibility criteria. A screw dislocation is invisible when $\boldsymbol{g}\cdot\boldsymbol{b} = 0$. An edge dislocation is invisible when $\boldsymbol{g}\cdot\boldsymbol{b} = 0$, and a residual contrast depends upon the angle between ***g*** and $\boldsymbol{b} \times \boldsymbol{l}$, where ***l*** is dislocation line direction. For a mixed dislocation, visibility is the lowest under the same conditions as for edge one, and the contrast corresponding to the $\boldsymbol{g}\cdot\boldsymbol{b}_e = 0$ criterion, where $\boldsymbol{b}_e$ – edge component of the mixed dislocation, is usually negligible.

The DF images shown in Fig. 1 were acquired under two-beam conditions with the diffraction vector $\boldsymbol{g} = 0006$ (*a*), $\boldsymbol{g} = \overline{1}\overline{1}20$ (*b*) and $\boldsymbol{g} = 0\overline{1}12$ (*c*). It can be seen that strong contrast is generated at the lowest number of TDs when $\boldsymbol{g} = \overline{1}\overline{1}20$ (Fig. 1, *b*). This result is inconsistent with previously published reports [5, 6, 11]. Furthermore, we classify the TDs imaged with the diffraction vector $\boldsymbol{g} = 0006$ (Fig. 1, *a*) as mixed perfect dislocations having non-zero $\boldsymbol{c}$-component and Burgers vector of $1/3 < 1\overline{1}00 >$. The majority of dislocations, observed at $\boldsymbol{g} = 0\overline{1}12$ (Fig. 1, *c*), should have a Burgers vector of $1/3 < 1\overline{1}00 >$, because we do not observe so many TDs under g = 0006. It is more likely that this contrast is caused by the many flat boundaries located in the layer.

Plan-view specimens were prepared to analyze the density and spatial distribution of dislocations. The specimens were taken not from the surface but from the volume of the film, since the lift-out method requires some space to prepare a lamella. The dislocation density was found to be not higher than 10^{10} cm^{-2}. Fig. 2 clearly shows images of plan-view specimens that contained dislocations and a large number of boundaries. The images were acquired along the [0001] zone axis, using a bright-field (BF) scanning TEM (STEM). To determine the location and shape of boundaries, each sample was tilted with respect to the incident electron beam. As a result, the inclined projections allowed us to reveal that a flat boundary was located perpendicular to the basal plane and terminated at dislocations. Most of the TDs are localized at the boundaries.

The presence of inclusion of 60°-rotational domains was also found out, but these inclusions could not form open boundaries. These inclusions should be bounded by prismatic domain boundaries, thus they can only explain the presence of closed boundaries.

a)
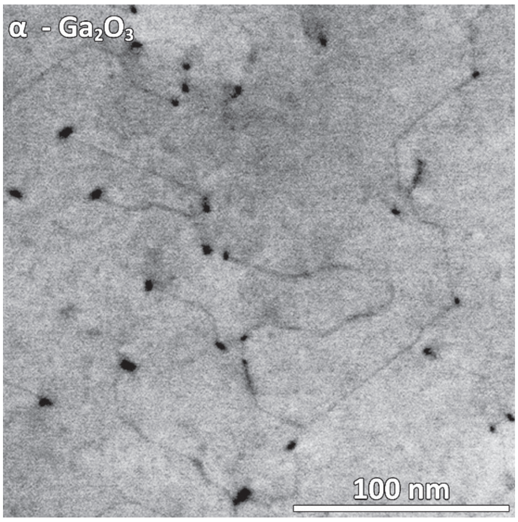

b)
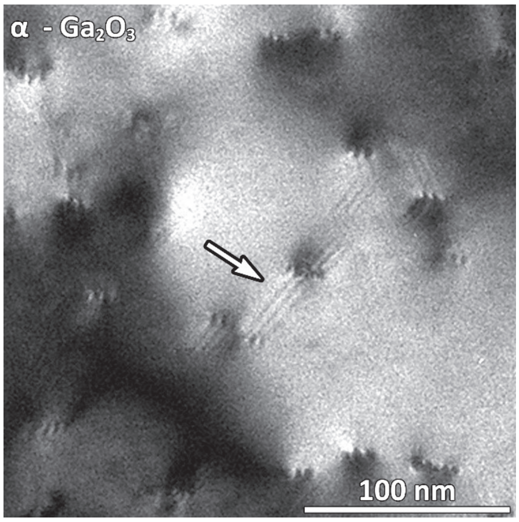

Fig. 2. Plan-view STEM-BF images taken along [0001] zone axis. Projections of the TD lines onto the basal plane. The occurrence and distribution of planar defects (located on prismatic planes) can be seen between the dislocations (*a*). A sample is tilted with respect to the incident electron beam. Multiple fringes that appeared on the image confirm the presence of prismatic faults (*b*)

It is known that perfect dislocation can dissociate into two partial dislocations because it lowers total energy. Such reactions have been studied for sapphire [13–15]. Below we consider stacking faults (SF), located at prismatic planes and terminated by partials. According to the images, shown in Fig. 2, the separation between the stacking faults is up to a few tens of nanometers.

The Burgers vectors of TDs were determined by a Burgers circuit procedure. Images of dislocation cores were acquired along the zone axis [0001] using high-resolution electron microscopy (HREM). Fig. 3, *a* shows two dislocation cores. Small Burgers circuits are drawn around each core. The core regions are associated with partial dislocations having the Burgers vectors $\boldsymbol{b}_2 = 1/3 < 1\overline{1}00 >$ and $\boldsymbol{b}_3 = 1/3 < 10\overline{1}0 >$. The inset of Fig. 3, *a* represents magnified fragments of a large Burgers circuit drawn around the pair of dislocations. It is seen that the extra atom-to-atom path corresponds to the Burgers vector $\boldsymbol{b}_1 = 1/3 < 2\overline{1}\overline{1}0 >$ of the perfect dislocation. This result is similar to earlier findings of the dislocation structures of low angle grain boundaries in sapphire [14]. The following dissociation reaction can be proposed: $1/3 < 2\overline{1}\overline{1}0 > \rightarrow 1/3 < 1\overline{1}00 > + 1/3 < 10\overline{1}0 > +$ SF, suggesting that the stacking fault on $\{2\overline{1}\overline{1}0\}$ prismatic plane is formed between partial dislocations. The plane of SF does not coincide with the slip plane of the perfect dislocation 1/3 < $2\bar{1}\bar{1}0$ >, as it is pointed out in [14]. Therefore, one should conclude that the self-climb mechanism takes place.

Our data show that neither inclusions of 60° rotational domains nor prismatic SFs appear against the background of the matrix in HREM-images along the [0001] zone axis. The large separation of stacking faults makes it difficult to trace and compare the paths between two partial dislocations.

The HREM-image in Fig. 3, *b* represents the core of either mixed perfect 1/3 < $1\bar{1}01$ > or partial 1/3 < $1\bar{1}00$ > TD. It should be noted that mixed perfect 1/3 < $1\bar{1}01$ > dislocations also have a 1/3 < $1\bar{1}00$ > component of the Burgers vector. We identified ten 1/3 < $1\bar{1}00$ > cores throughout the investigations of the HREM-images acquired along the [0001] zone axis.

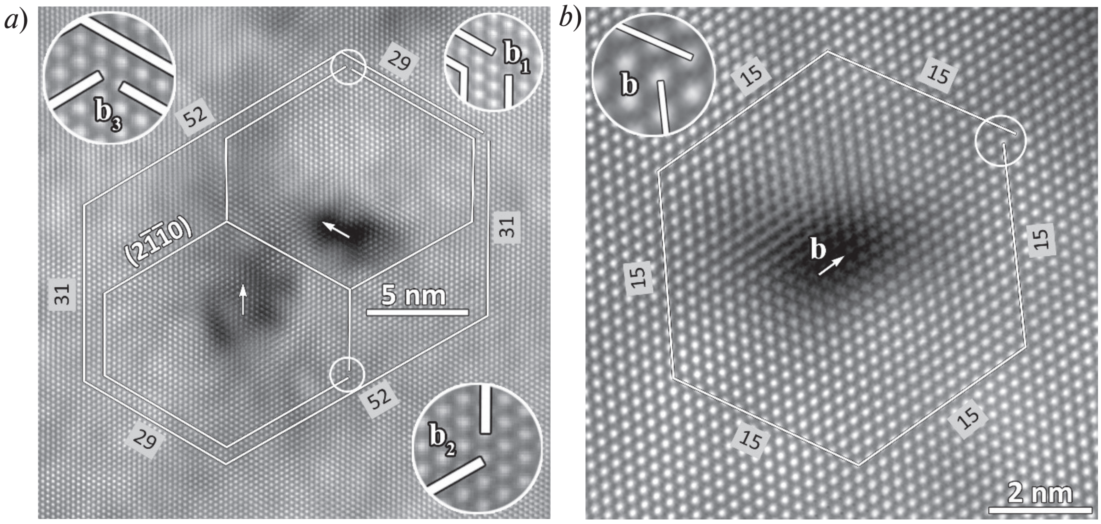

Fig. 3. Fourier-filtered HREM-images of dislocation cores were acquired along the zone axis [0001]. Two dislocation cores are located next to each other. A large Burgers circuit shows the edge component of $\boldsymbol{b}_1$ = 1/3 < $2\bar{1}\bar{1}0$ >. A small Burgers circuits show the edge components of $\boldsymbol{b}_2$ = 1/3 < $1\bar{1}00$ > and $\boldsymbol{b}_3$ = 1/3 < $10\bar{1}0$ > (*a*). Single dislocation core with Burgers vector $\boldsymbol{b}$ = 1/3 < $01\bar{1}0$ >. The inserts show enlarged areas of the extra atom-to-atom path of the Burgers circuit drawn around dislocation cores (*b*)

Conclusion

The dislocation structure of α-Ga_2O_3 films grown on Al_2O_3 (0001) substrates by HVPE has been investigated using conventional and high-resolution TEM methods. The films contained a very large quantity of TDs with a density of about 10^{10} cm^{-2}. The density of mixed-type dislocations was not much less than that of edge TDs. The Burgers vector of the majority of dislocations were identified as 1/3 < $1\bar{1}00$ >. Furthermore, our study revealed that edge TDs tend to dissociate into partial dislocations bounding prismatic stacking faults. High strain resulted in the formation of flat boundaries, rotational domains, and stacking faults, which deteriorated the crystalline quality.

REFERENCES

1. **Zhang J., Shi J., Qi D.-C., Chen L., Zhang K.H.L.,** Recent progress on the electronic structure, defect, and doping properties of Ga_2O_3, APL Mater. 8 (2) (2020) 020906.

2. **Ahmadi E., Oshima Y.,** Materials issues and devices of α- and β-Ga_2O_3, J. Appl. Phys. 126 (16) (2019) 160901.

3. **Oshima Y., Vнllora E.G., Shimamura K.,** Halide vapor phase epitaxy of twin-free α-Ga_2O_3 on sapphire (0001) substrates, Appl. Phys. Express. 8 (5) (2015) 4–8.

4. **Stepanov S.I., Nikolaev V.I., Almaev A.V., Pechnikov A.I., Scheglov M.P., Chikiryaka A.V., Kushnarev B.O., Polyakov A.Y.,** HVPE growth of corundum-structured α-Ga_2O_3 on sapphire substrates with α-Cr_2O_3 buffer layer, Cryst. Growth Des. 47 (2021) 577–581.

5. **Kaneko K., Kawanowa H., Hiroshi I., Fujita S.,** Evaluation of misfit relaxation in α-Ga_2O_3 epitaxial growth on α-Al_2O_3 substrate, Appl. Phys. 51 (2012) 020201.
6. **Ma T.C., Chen X.H., Kuang Y., Li L., Li J., Kremer F., Ren F.-F., Gu S.L., Zhang R., Zheng Y.D., Tan H.H., Jagadish C., Ye J.D.,** On the origin of dislocation generation and annihilation in α-Ga_2O_3 epilayers on sapphire, Appl. Phys. Lett. 115 (18) (2019) 182101.
7. **Fujita S., Oda M., Kaneko K., Hitora T.,** Evolution of corundum-structured III-oxide semiconductors: Growth, properties, and devices, Jpn. J. Appl. Phys. 55 (12) (2016) 1202A3.
8. **Yamaguchi H., Kuramata A., Masui T.,** Slip system analysis and X-ray topographic study on β-Ga_2O_3, Superlattices Microstruct. 130 (2019) 232.
9. **Yao Y., Sugawara Y., Ishikawa Y.,** Observation of dislocations in β-Ga_2O_3 single crystal substrates by synchrotron X-ray topography, chemical etching, and transmission electron microscopy, Jpn. J. Appl. Phys. 59 (4) (2020) 045502.
10. **Pechnikov A.I., Stepanov S.I., Chikiryaka A.V., Scheglov M.P., Odnobludov M.A., Nikolaev V.I.,** Thick α-Ga_2O_3 layers on sapphire substrates, grown by halide epitaxy, Semiconductors. 53 (6) (2019) 780–783.
11. **Oshima Y., Yagyu S., Shinohe T.,** Visualization of threading dislocations in an α-Ga_2O_3 epilayer by HCl gas etching, J. Cryst. Growth. 576 (2021) 126387.
12. **Snow J. D., Heuer A. H.,** Slip Systems in Al_2O_3, J. Am. Ceram. Soc. 56 (3) (1973) 153–157.
13. **Lagerlkf K.P., Mitchell T.E., Heuer A.H.,** TEM of dislocations in sapphire (c-Al_20_3), 31 (1984) 303–315.
14. **Tochigi E., Nakamura A., Shibata N., Ikuhara Y.,** Dislocation structures in low angle grain boundaries of α-Al_2O_3, Crystals. 8 (3) (2018) 1–14.
15. **Tsuruta K., Tochigi E., Kezuka Y., Takata K., Shibata N., Nakamura A., Ikuhara Y.,** Core structure and dissociation energetics of basal edge dislocation in α-Al_2O_3: A combined atomistic simulation and transmission electron microscopy analysis, Acta Mater. 65 (2014) 76–84.

THE AUTHORS

MYASOEDOV Alexander V.
amyasoedov88@gmail.com
ORCID: 0000-0003-2706-7240

STEPANOV Sergey I.
s.i.stepanov@gmail.com
ORCID: 0000-0003-1324-3055

PAVLOV Ivan S.
win8765495@gmail.com
ORCID: 0000-0001-9366-0101

NIKOLAEV Vladimir I.
Nikolaev.V@mail.ioffe.ru
ORCID: 0000-0002-5630-0833

PECHNIKOV Aleksey I.
pechnikovai@gmail.com
ORCID: 0000-0003-4604-1935

Received 28.09.2022. Approved after reviewing 10.11.2022. Accepted 17.11.2022.